ISSN (Print) 1226-1750
ISSN (Online) 2233-6656
Journal of Magnetics 22(1), 122-132 (2017) https://doi.org/10.4283/JMAG.2017.22.1.122

Design and Characteristics Analysis of the 78 kWe Grade Synchronous Generator for Disused Diesel Engines

Jun-Seop Youn, Hae-Joong Kim, Youn-Hwan Kim, and Jae-Won Moon*

Rotating Machinery Center, Korea Testing Certification, 22, Heungan-daero 27beon-gil, Gunpo-si, Gyunggi-do 15809, Korea

(Received 28 July 2016, Received in final form 24 January 2017, Accepted 26 January 2017)

This study dealt with the design process of the 78 kW permanent magnet synchronous generator for engines. After the calculation of the basic dimensions through a theoretical method in the process of initial model design, FEA (finite-element analysis) and a d,q-axis equivalent circuit were used to identify the generator characteristics depending on the number of poles. With the use of the space harmonic analysis method, the back-EMF (electromotive force) and THD were checked, and then the number of slots was determined. In addition, the most optimized generator dimensions were determined through a sizing optimization technique. Based on this, the optimum model with enhanced efficiency, material costs, and temperature characteristics was derived, and the availability of the design method was confirmed through a comparative analysis of the initial and optimum models.

Keywords : synchronous generator, sizing, permanent magnet, efficiency, space harmonic analysis

1. Introduction

With the gradual increase in population inflow into the downtown area, the power consumption increase and electric power system is becoming complex. For this reason, a diesel generator has been widely used for emergency power generation in buildings, factories, and hospitals, and especially for island operation in the central part of the city. This is because there is limited power supply through the existing distribution lines, and the installation costs are large. The use of the diesel generator has disadvantages, such as the fact that it cannot be operated at all times and causes environmental pollution, a rise in fuel prices, and large noise problems, but it also has advantages, such as the fact that it can shorten the power supply time and ensure convenience and a broad range of applications. Despite the advantages of the use of the diesel generator, however, as various problems have emerged of late owing to environmental pollution, situations that necessitate a reduction of the fuel gas emissions and energy consumption by lowering the installation costs and raising the efficiency of the diesel generator have emerged. In this regard, this study dealt with the design process of the diesel engine generator made by remanufacturing the waste engine whose number of discharges is currently more than 750,000 per year but whose residual value remains more than 50 % [1-3].

The capacity is 79 kWe-grade, and the rated torque and rated speed were determined considering the operating speed and output of the engine. In the initial model design process, the required power factor and required voltage regulation were determined based on the regulations of the International Organization for Standardization (ICS). The shaft diameter was calculated by considering the tensile stress and tensile strength. The PM (permanent magnet) that was used in the generator was a rare earth material, and the rare-earth PM has the characteristics of a high coercive force and a high residual magnetic flux density. In calculating the basic dimensions of the generator, the TRV (torque per rotor unit volume) and SR (shape ratio) were used, and the tooth width, yoke width, and pole angle were determined via FEA. To determine the number of poles, the inductance, EMF THD, and iron loss of the generator were compared, and the characteristics were analyzed using FEA and a d,q-axis equivalent circuit. The EMF waveforms induced by the number of slots were compared using the space harmonic analysis method to determine the number of slots. With respect to the initial model designed this way, the final optimum model was obtained by finding the optimal TRV and SR

©The Korean Magnetics Society. All rights reserved.
*Corresponding author: Tel: +82-31-428-3766
Fax: +82-31-455-7236, e-mail: yunjunsup@ktc.re.kr

© 2017 Journal of Magnetics

values with the use of the sizing optimization technique.

2. Initial Design of a Generator

2.1. Setting a Basic Specification

First, the basic specifications of the generator were set. The types of generator include the induction generator, wound rotor synchronous generator, and permanent-magnet synchronous generator (PMSG), and among these, PMSG was selected because it has not only the smallest voltage regulation and frequency regulation but also a better power density and efficiency. With regard to the generator speed, in the case of a vehicle engine, the rated speed is 1800 rpm in general, and as such, the same value was set as the input speed of the generator. According to the national and international standards and classifications societies, the main boundary conditions for an SG for island AC operation are generally the 0.9/1.1 U_{ph} terminal voltage range in normal operation, $\geq 3I_n$ sustainable short-circuit current, and 0.8 power factor, and based on these, the value was selected as shown in Table 1 [4-7]. As for the input torque, 460 Nm, the torque value at the 78 kW output and 1800 rpm speed, was selected, and 0.8 was applied as a load power factor, and the natural air cooling system as the cooling system.

$$P = T \times \omega_m \tag{1}$$

2.2. Calculation of the Number of Poles and Slots on a Generator

The initial values for determining the dimensions and size of the generator were selected. For the TRV and SR, the initial values were planned to be set theoretically and then to be reset through the sizing technique. The initial TRV value was set to 60, and equation (2) was used. σ_{mean} is the share stress that was applied to the rotor, and its unit is kNm/m^3.

$$TRV = 2\sigma_{mean} \tag{2}$$

Table 1. Design requirements.

Parameters	Value	Unit
Generator type	SPMSG	–
Rated Power	78	kW
Rated Speed	1800	rpm
Rated Torque	460	Nm
Line Voltage	380	V_{rms}
Voltage regulations	≤10	%
Output Frequency	60	Hz
Power factor (loaded)	0.8	–
Cooling Type	Natural cooling method	–

Table 2. Main geometry.

Parameters	Value	Unit
TRV	60	kNm/m^3
Shape Ratio	1	–
Slot coil space factor	35	%
Current density	4	A_{rms}/mm^2
Shaft diameter	80	mm

N42SH was used as a permanent magnet, 50PN470 as a magnetic core, and the SM45C material for the shaft. Considering the tensile stress and tensile strength, the thickness was determined to be 80 mm in the initial stage. The SR is the value obtained by dividing the stack length by the rotor outer diameter. In this study, it was determined to be 1 but was scheduled to be adjusted based on the results of a detailed analysis. Given the performance of the generator, an about 45 % higher slot fill factor needs to be applied, but it was set to 35 % in the initial design considering the production convenience. The rotor volume can be calculated by dividing the rated torque by the TRV, and the rotor volume of the initial model was determined to be 0.0077 m^3. The rotor outer diameter was determined using the following equation, and it was calculated to be 214 mm for the 4-pole generator and 290 mm for the 8-pole generator. In addition, the current density was determined to be 4A rms/mm^2, and a void pole was set at 1 mm, as shown in Table 2.

$$\sqrt{\frac{\pi}{4} \times \frac{\text{Rotordiameter}}{\text{Shape Ratio}}} \tag{3}$$

2.2.1. Determination of the number of poles on a generator

The number of poles on a generator was selected by considering the operating speed of the engine. Based on 60 Hz, the 4-pole generator runs at 1800 rpm, the 6-pole generator at 1200 rpm, and the 8-pole generator at 900 rpm. As the rated operating speed of the engine is 1800 rpm, a gear has to be applied when designing a 6- or 8-pole generator. In this study, a comparative analysis was conducted to check which number of poles ensures less THD, iron loss, and inductance. To determine the performance variation depending on the number of poles, a comparative analysis of the 4- and 8-pole generators was conducted. The number of slots was proportional to the number of poles, as in 24 slots for the 4-pole generator and 48 slots for the 8-pole generator, and Fig. 1 shows a model designed based on these values.

Table 3 compares the values from the shapes of the 4-pole/24-slot and 8-pole/48-slot models. The tooth and yoke widths were designed to ensure that the flux density

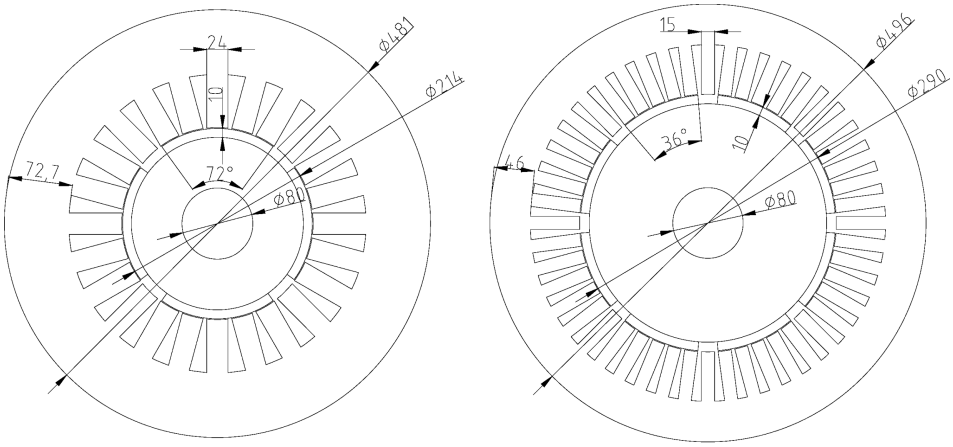

(a) 4pole-24slot model (b) 8pole-48slot model

Fig. 1. The (a) 4pole-24slot and (b) 8pole-48slot model.

Table 3. The comparison of the dimension of the 4-pole/24-slot and 8-pole/48-slot models.

Parameters	4pole 24slots	8pole 48slots	Unit
Stator external diameter	481	496	mm
Rotor external diameter	214	290	mm
Stack length	214	290	mm
Tooth/Yoke width	24/72.7	15/46	mm
Permanent Magnet Thickness	10	10	mm
Pole angle	72	36	deg.
Rotor diameter	36	40	mm
Volume	0.0389	0.0561	m^3

becomes 1.2 T. As the cogging torque and no-load-induced EMF THD showed a tendency to decrease at around the 0.8 pole angle ratio, the pole angle was selected accordingly. For the number of series turns per phase, the required terminal voltage is 220 V_{rms}; therefore, it was determined so that the no-load-induced voltage can become 250 V_{rms} considering the voltage drop. An analytical method was used when deciding the no-load-induced voltage.

2.2.1.1. FEA for Calculating the Number of Poles

To determine the number of poles, the 4-pole and 8-pole models were analyzed under the same conditions (temperature = 100°C and Br = 1.2 T). FEA was used in the calculation of the no-load-induced voltage, inductance, and iron loss. Figure 2 shows the comparison of No-load voltages and its THD of 4pole with 8pole model and it shows no-load-induced voltages were almost same but THD of 4pole model (12.3 %) was better than 8pole (15.6 %). The iron loss was analyzed in the phase resistance = 2.11 Ω rated load conditions. Under the same conditions, the 4-pole model's phase induced voltage and d,q-axis inductance were relatively higher than those of the 8-pole model. On the other hand, the iron loss and induced-voltage THD of the 4-pole model turned out to be 30.8 % and 3.3 %, respectively. The reason that the 4-pole model has a relatively large inductance is that its cross-sectional area is wider than that of the 8-pole model. Table 4 compares the result values.

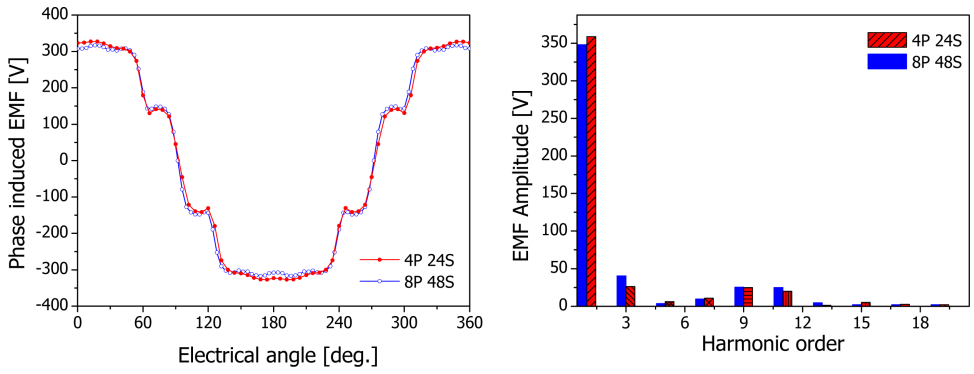

(a) Phase induced EMF(No load) (b) EMF Amplitude

Fig. 2. (Color online) The (a) phase induced EMF and (b) EMF Amplitude of the 4pole-24slot and 8pole-48slot.

Table 4. The result of FEA for calculating the number of poles.

Parameters	4pole 24slots	8pole 48slots	Unit
Speed	1800	900	rpm
Power	78	78	KW
Phase induced EMF (No load)	253.6	246.0	V_{rms}
THD	12.3	15.6	%
L_d, L_q	2.0	1.3	mH
Iron loss	654	945	W_i
Phase wire wound resistance	0.034	0.033	Ω
Power factor (Load)	1	1	

2.2.1.2. Analysis of the Generator Characteristics for Calculating the Number of Poles

For the analysis of the generator characteristics, a d,q-axis equivalent circuit was used. The iron loss resistance (R_c) was calculated using equation (4). The generator characteristics were determined by applying the generator parameters, such as the induced voltage, inductance, phase resistance, and iron loss resistance, to the d,q-axis equivalent circuit. In the following equation (4), the iron loss resistance (R_c) value is inversely proportional to the iron loss (W_i), and proportional to the square of the load-induced voltage. As it is difficult to apply the load-induced voltage to equation (4), a no-load-induced voltage was applied in this study. In the q-axis equivalent circuit shown in Fig. 3(b), $\omega\psi_a$ is the no-load-induced voltage.

$$R_c = \frac{V_a^2}{W_i} \approx \frac{E_a^2}{W_i} \tag{4}$$

Using the d,q-axis equivalent circuit, a graph showing the changes in the line-to-line voltage and the output power for the 4- and 8-pole models were obtained. A look at the current-voltage graph in Fig. 4(a) can confirm that when the output power increases, the terminal voltage of the 4-pole model drops more rapidly than that of the 8-pole model. Both the 4- and 8-pole models, however, have no difficulty securing the rated output power under the rated load condition. The current-power graph in Fig. 4(b) reveals that both the 4- and 8-pole models can exert the target power of more than 78 kW under the condition of load power factor 1.

The above result values are presented in Table 5. The voltage regulation of the 4-pole model turned out to be higher than that of the 8-pole model. This is because the pole of the 4-pole model has a greater cross-sectional area than that of the 8-pole model, and thus, the inductance value is also large. Although the 4-pole model has the disadvantage of having large voltage regulation, it has a greater power density than the 8-pole model, indicating the possibility of reducing the material costs. Therefore, the 4-pole model was adopted, and attempt was made to

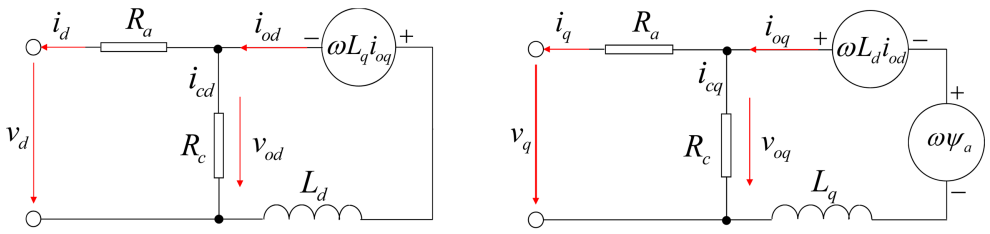

(a) d-axis equivalent circuit (b) q-axis equivalent circuit

Fig. 3. (Color online) The (a) d-axis and (b) q-axis equivalent circuit.

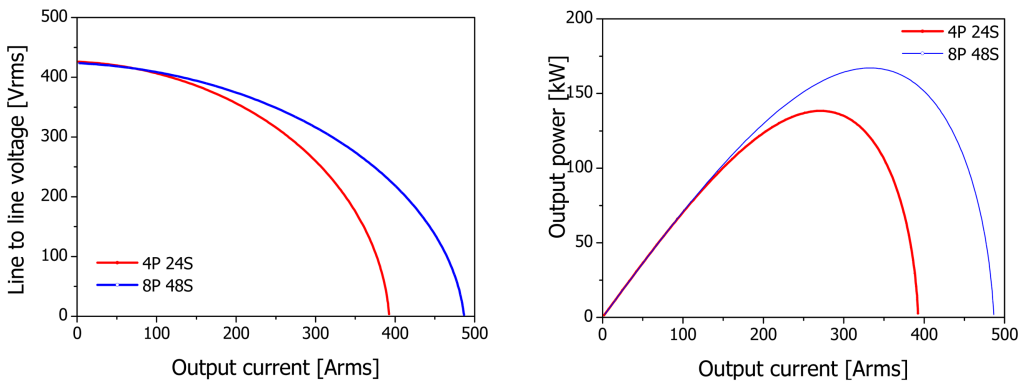

(a) The line voltage of two models (b) The output power of two models

Fig. 4. (Color online) The (a) line voltage and the (b) output power of the 4pole-24slot and 8pole-48slot model.

Table 5. The result of analysis of the generator characteristics for calculating the number of poles.

Parameters	4pole 24slots	8pole 48slots	Unit
Speed	1800	900	rpm
Line voltage	402.0	406.0	V_{rms}
Load current	113.0	110.0	A_{rms}
Efficiency	97.6	97.4	%
Voltage regulation	8.4	4.7	%

improve its voltage regulation through the inductance reduction design.

2.2.2. Determination of the number of slots on a generator

Next, space harmonic analysis was conducted to determine the number of slots, and the results are summarized in Fig. 5 and Table 6. The no-load-induced EMF THD was found to be relatively low in 27, 30, 33, 39, and 42 slots, and the radial force order (r_λ) value was higher in 8, 24, 30, 36, and 42 slots. The deformation of a stator is inversely proportional to the fourth power of the radial force order (r_λ) value, which means that as this value increases, the deformation of the stator decreases. A comparison of the above values leads to the expectation that 42 slots will show excellent EMF THD and vibration performance characteristics. Accordingly, 42 slots were determined as the number of slots for the initial model.

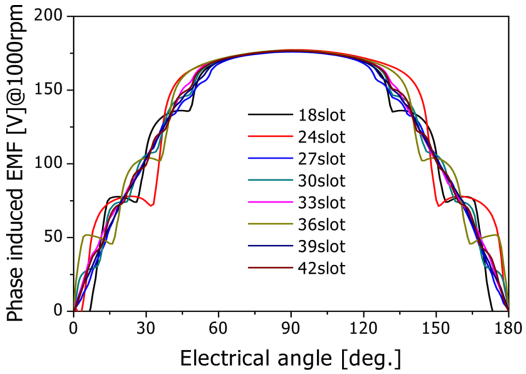

Fig. 5. (Color online) The phase induced EMF depending on the changes of the number of slots (analysis result from space harmonic analysis method).

Table 6. The comparison of the parameters according to the number of slots (analysis result from space harmonic analysis method).

The number of Slots	Phase induced EMF (No load)	EMF THD	Radial force order
18	190.2	9.3	4
24	195.1	13.4	4
27	189.4	6.2	2
30	191.7	7.7	4
33	192.6	7.5	2
36	193.8	11.1	4
39	191.0	6.8	2
42	192.3	7.4	4

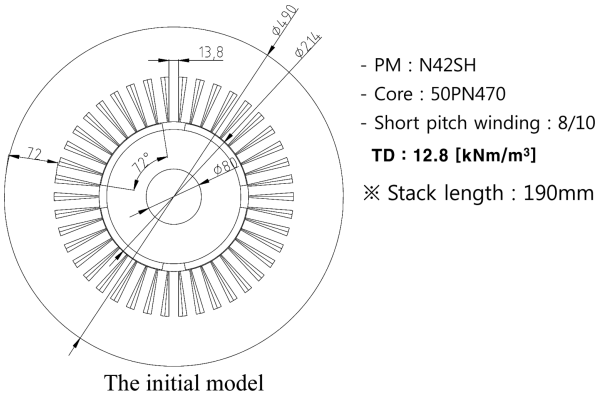

Fig. 6. The shape of the initial model.

2.2.3. Shape of the initial model

Based on the above result values, the 4-pole/48-slot model was designed as shown in Fig. 6. The stator outer diameter was 490 mm, the rotor outer diameter was 214 mm, the pole angle was 72°, the shaft diameter was 80 mm, the tooth width was 13.8 mm, and the yoke width was 72 mm. While increasing the slot fill factor from 35 to 45 %, the stack length was reduced by 100 mm, and the stator outer diameter increased by 10 mm. As a result, the volume of the generator was reduced by 8 %, from 0.0389 to 0.0358 W/cm^3. Table 7 shows the parameters of the 4-pole generator with 48 slots. The volume was reduced while the previously used slot fill factor was changed from 35 to 45 %, the TRV was changed from 60 to 67, and the SR was changed from 1 to 0.887 in the process.

Table 7. The parameters of the initial model.

Parameters	4pole 42slots	Unit
Rated Speed	1800	rpm
Rated Power	78	kW
Phase induce EMF (No load)	244.1	V_{rms}
EMF THD	3.7	3.7
L_d, L_q	2.2	mH
Iron loss	595	W
Phase wire wound resistance	0.033	Ω
Power density	2.17	W/cm^3
Slot coil space factor	45	%
TRV	67	kNm/m^3
Shape Ratio	0.887	–

3. Design through the Sizing Optimization Technique

3.1. Sizing optimization

The values to be ultimately obtained through the sizing optimization technique in this study included the stator outer diameter (D_s), rotor outer diameter (D_r), and stack length (L_{stack}). These values were determined through the SR, torque density (TD), and TRV selected at the time of the initial design, and they were the results that were obtained using the following equation:

$$TRV = \frac{T_{\max}}{\text{Rotor unit Volume}} = \frac{T_{\max}}{\frac{\pi}{4}D_r^2 L_{stack}} \tag{5}$$

$$\text{Shape ratio (SR)} = \frac{L_{stack}}{D_{rotor}} \tag{6}$$

$$\text{Torque Density (TD)} = \frac{T_{\max}}{\text{Volume}} = \frac{T_{\max}}{\frac{\pi}{4}D_s^2 L_{stack}} \tag{7}$$

Through the above equation, *TRV*, *SR*, and *TD* were found to have D_s, D_r, and L_{stack} values as variables. Thus, the D_s, D_r, and L_{stack} values can be represented, respectively, by the following equations that have *TRV*, *SR*, and *TD* as variables:

$$D_s(TRV, TD, SR) = \sqrt{\frac{T_{\max}}{\frac{\pi}{4}\times TD_s \times \frac{T_{\max}\times SR^2}{\frac{\pi}{4}TRV}}} \tag{8}$$

$$D_r(TRV, SR) = \sqrt{\frac{T_{\max}}{\frac{\pi}{4}\times TRV \times SR}} \tag{9}$$

$$L_{stack}(TRV, SR) = \sqrt{\frac{T_{\max}\times SR^2}{\frac{\pi}{4}\times TRV}} \tag{10}$$

Figure 7 shows a graph representing the above equations. The stator outer diameter (D_s) shows a tendency to decrease as the *SR* increases, but to increase as the *TRV* increases. The rotor outer diameter (D_r) shows a tendency to decrease with an increase in the SR, and to be reduced as the *TRV* increases. The stack length (L_{stack}) shows a tendency to increase with an increase in the *SR*, but to decrease with an increase in the *TRV*.

As mentioned earlier, it was decided that the inductance be decreased so as to reduce the voltage regulation of the generator. Prior to reducing the inductance, the generator characteristics needed to be analyzed using a d,q-axis equivalent circuit. In the d,q-axis equivalent circuit in Fig. 3, the generator parameters had to be known to be able to determine the $i_{d,q}$, $v_{d,q}$, R_a, R_c, L_d, L_q, and $\omega\psi_a$ values, and to determine the generator parameters, the tooth width (T_{tooth}), yoke width (T_{yoke}), slot area (A_s), and series turns per phase (N_s) should first be known. These values can be represented by the equation that has D_s, D_r, and L_{stack} as variables, and the equations regarding *TRV*, *SR*, and *TD* can be represented as the equations below.

$$T_{tooth}(D_r) = T_{tooth}(TRV, SR) = \frac{B_g\pi}{B_t S}D_r \tag{11}$$

$$T_{yoke}(D_r) = T_{yoke}(TRV, SR) = \frac{B_g\pi}{4B_y P}D_r \tag{12}$$

$$A_s(D_s, D_r) = A_s(TRV, TD, SR) = \frac{\pi}{4S}\{(D_s - 2T_{yoke})^2 - D_r^2\} - \frac{T_{tooth}}{2}(D_s - 2T_{yoke} - D_r) \tag{13}$$

$$N_s(D_r, L_{stack}) = N_s(TRV, SR) = \frac{\pi}{2D_r}\frac{P}{\omega k_w E_a L_{stk} B_g} \tag{14}$$

$$E_a = \omega\psi_a \tag{15}$$

$$R_a(D_r, D_s, L_{stack}) = R_a(TRV, TD, SR) = \rho\frac{L_c N_s}{A_c} \tag{16}$$

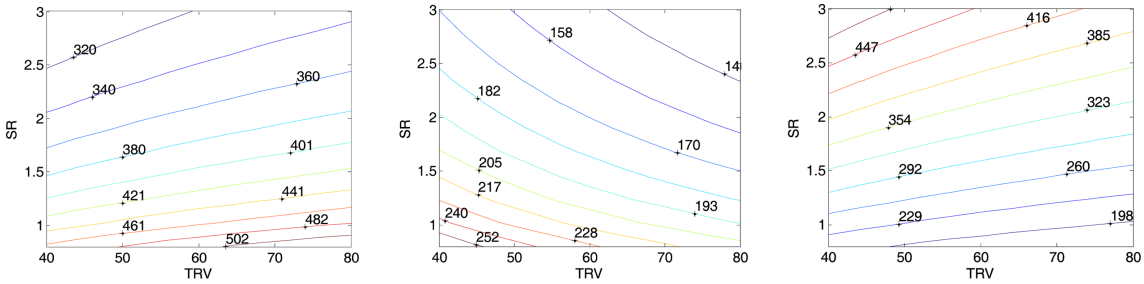

(a) Stator diameter [mm] (b) Rotor diameter [mm] (c) Stack length [mm]

Fig. 7. (Color online) The (a) Stator diameter, (b) Rotor diameter and (c) Stack length depending on the changes in the TRV and SR.

$$L_{d,q}(D_r, L_{stack}) = L_{d,q}(TRV, TD, SR) = \frac{3}{\pi}\mu_0\left(\frac{k_w N_s}{P}\right)^2 \frac{D_r L_{stk}}{g} \quad (17)$$

$$R_c(D_s, L_{stack}) = R_c(TRV, TD, SR) = \frac{V_0^2}{W_i} \approx \frac{3E_a^2}{\omega D_s^2 L_{stk}\pi/2} \quad (18)$$

The air flux density, is B_g, the toothe flux density is B_t, the yoke flux density is B_y, the load back EMF is V_0, the iron loss is W_i, the air gap length is g, the winding factor is k_w, the number of pole pair is P, the number of slots is S, the copper length is L_c, the copper area is A_c, and the no-load back EMF is E_a unchanged in the changes of *TRV*, *TD* and *SR*.

Sizing optimization after the changes of *TRV*, *TD* and *SR* is available, for the shape of generator, equation (11)-(14) was used and for the generator characteristics, a d,q-axis equivalent circuit by parameters from equation (15)-(18) was used.

The above R_a, R_c, and L_{stack} values can be used to obtain the input voltage, loss, and efficiency. If these values are changed into variables on the *TRV*, *SR*, and *TD*, and represented in a graph, the input voltage, loss, and efficiency depending on the changes in the *TRV*, *SR*, and *TD* can be identified. Figure 8 shows a graph based on the input voltage, loss, efficiency, winding temperature, and material cost. The *TD* was set to a fixed value, and only the SR and TRV were compared. The inductance shows a tendency to decrease with an increase in the *SR*, but to increase with an increase in the *TRV*. The efficiency tends to increase as both the *SR* and *TRV* increase. The material cost shows a tendency to increase as the *SR* increases, but to decrease as the *TRV* increases. The winding temperature shows a tendency to decrease as both the *SR* and *TRV* increase.

The blue dotted line in the graph is a line that connects the point where the outer diameter of the rotor is 200 mm. To ensure that the maximum density value of the rotor is less than 1.5 T, the outer diameter of the rotor should be at least 200 mm or more. Therefore, the *TRV* and *SR* values had to be determined based on the blue dotted line in the graph.

As mentioned earlier, the objective of the optimization process is to reduce the inductance, and thus to lower the

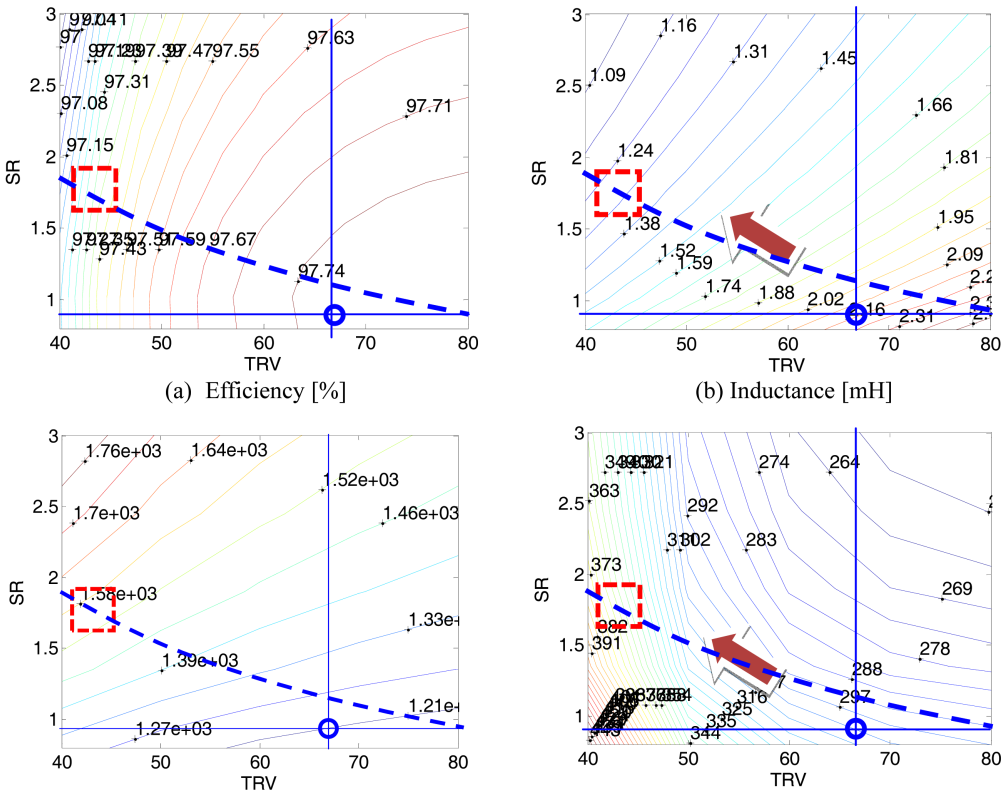

(a) Efficiency [%]

(b) Inductance [mH]

(c) Cost of material [USD]

(Unit cost of Nd: $90[USD/kg], Unit cost of copper: $12[USD/kg], Unit cost of core: $1.3[USD/kg])

(d) Temperature of end-coil [℃]

Fig. 8. (Color online) The (a) efficiency, (b) inductance, (c) cost of material and (d) Temperature of end-coil depending on the changes in the TRV and SR.

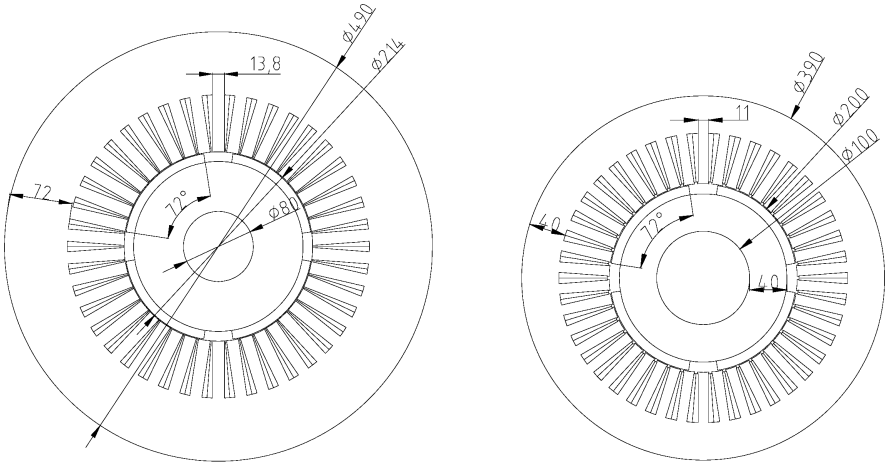

(a) The initial model (b) The optimum model

Fig. 9. The (a) initial and (b) optimum model.

Table 8. The comparison of the result of sizing optimization method and FEA (optimized model).

Parameters	Sizing optimization method	FEA	Unit
Phase induce EMF (No-load) @1800rpm	265	274.1	V_{rms}
L_d, L_q	1.3	1.5	mH
Iron loss	955	1064	W

Table 9. The comparison of the initial and optimum models.

Parameters	Initial model	Optimized (Sizing) model	Unit
Rated Speed	1800	1800	rpm
Rated Power	78	78	kW
Phase induce EMF (No load)	244.1	274.1	V_{rms}
EMF THD	3.7	3.4	%
L_d, L_q	2.2	1.5	mH
Iron loss	595	1064	W
Phase wire wound resistance	0.033	0.016	Ω
Power density	2.17	1.87	W/cm^3
Slot coil space factor	45	45	%
Stator external diameter	490	390	mm
Cost of material	1210	1550	USD
Rotor external diameter	214	200	mm
Stack length	190	350	mm
Tooth/Yoke width	13.8/ 72	11/ 40	mm
Permanent magnet thickness	10	10	mm
Pole angle	72	72	Deg.
Shaft diameter	80	100	mm
Volume	0.0359	0.0417	m^3
TRV	67	42	kNm/m^3
Shape Ratio	0.887	1.75	–

voltage regulation. Therefore, this study sought to find the optimum value based on the inductance graph. The inductance value shows a tendency to decrease as it pushes leftward along the blue dotted line. In this study, the point where the *SR* is 1.75 and the *TRV* is 42 was selected because the performance of the generator is affected by a rise in the material cost and an increase in the end winding temperature as it goes further to the left.

Furthermore, The comparison of the result of sizing optimization method and FEA is added to Table 8 to make sizing optimization method obvious and prove its reliability.

Figure 9 and Table 9 compare the initial model and the final model (sizing model) designed through the sizing optimization method. With the changes in the *TRV* and SR, the stator outer diameter was reduced by 100 mm, and the rotor outer diameter by 14 mm, but the stack length was increased by 160 mm. Finally, a look at the change in the volume can reveal that the volume of the optimum model was increased by about 16 % compared to that of the initial model.

4. Comparative Analysis of the Initial and Optimum Models

The results of the comparison of the initial and optimum models are as follows. First, the no-load-induced voltage was increased by 12.8 %, from 244.1 to 275.4 V_{rms}, and the THD was decreased by 0.3 %, from 3.7 to 3.4 %. In addition, the average inductance was decreased by 0.7 mH, from 2.2 to 1.5 mH.

In the cases where the load power factors of the initial and final models were 1 and 0.8, respectively, Fig. 11 shows a graph representing the generator output of the

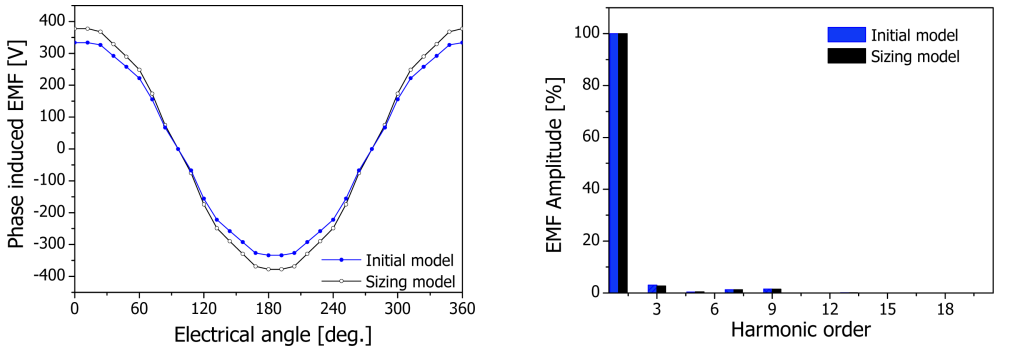

(a) The phase induced EMF(No load) (b) The EMF amplitude of the initial model

Fig. 10. (Color online) The (a) Phase induced EMF and (b) EMF amplitude of the initial and optimum model.

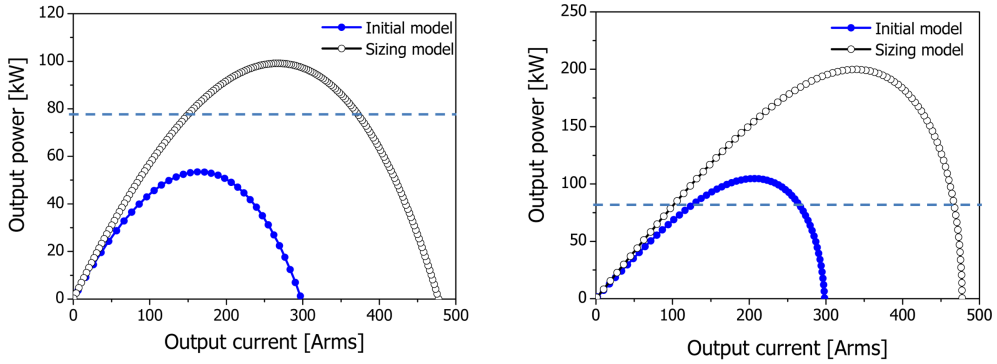

(a) The output power at p.f. 0.8 (b) The output power at p.f. 1

Fig. 11. (Color online) The output power of the initial and optimum model at (a) power factor 0.8 and (b) power factor 1.

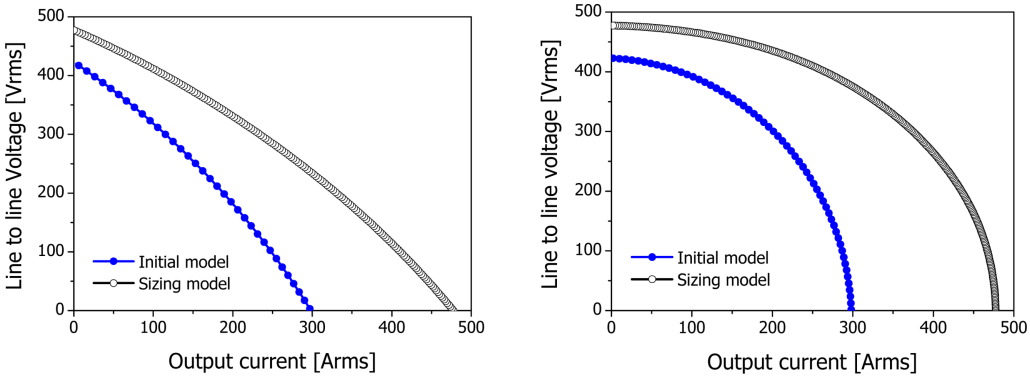

(a) The line voltage at p.f. 0.8 (b) The line voltage at p.f. 1

Fig. 12. (Color online) The line voltage of the initial and optimum model at (a) power factor 0.8 and (b) power factor 1.

initial and final models in the cases of load power factor 0.8(a) and load power factor 1(b). It can be confirmed that the final model can provide a target output in the case of load power factor 0.8, and that both the initial and final models can provide the target output in the case of load power factor 1. Figure 12 shows a graph representing the terminal voltages of the initial and final models in the cases of load power factor 0.8(a) and load power factor 1(b). It can be seen that the voltage regulation of the initial and final models was improved in both cases (load power factors 0.8 and 1). In the case of load power factor 1, the efficiency was similar, and the power density showed only a slight drop, but it can be confirmed that the voltage regulation of the initial model was 9.9 %, and that of the final model was 2.1 %, showing a 7.8 % decrease.

Figure 13 shows a graph representing the output power

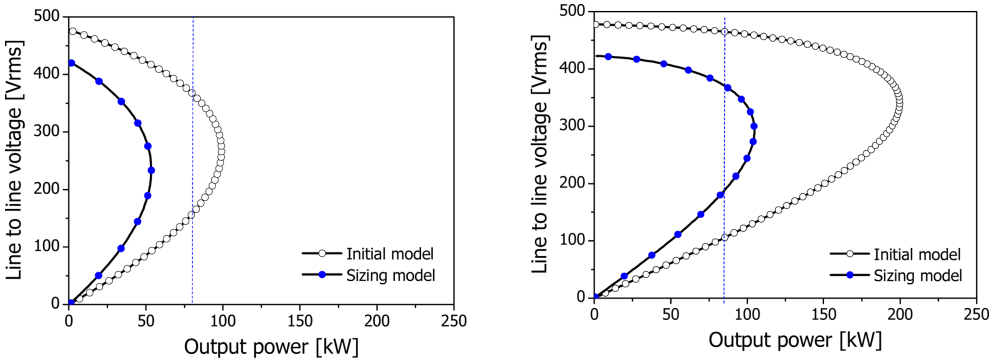

(a) The output & line voltage at p.f. 0.8 (b) The output & line voltage at p.f. 1

Fig. 13. (Color online) The output power and line voltage of the initial and optimum model at (a) pf 0.8 and (b) pf 1.

and line voltage in the cases of load power factor 0.8(a) and load power factor 1(b). it can be confirmed that as the line voltage goes up.

At last, as for the vibration and the bending of optimum model have been proved safety as follow. If bending moment occurred to center of a shaft which has bearings at its both ends in a normal rotating machine, the maximum bending(δ) and a diameter of shaft(d) has a relation as follow equation (19)

$$d = \sqrt[4]{\frac{4Wl^3}{3E\pi\delta}} \tag{19}$$

In this paper, the calculation has been done in follow conditions, the weight(W) to a shaft is 200[kgf], the length(l) is 800[mm], the diameter is 100[mm], the modulus of longitudinal elasticity(E) is 21,000[kg/mm^2]. As a result, the value of the maximum bending is 0.02 [mm] and 0.04[mm/m] and has been proved satety that's why the maximum bending is normal enough; the range of it in rotating machine in general must be below than 0.30[mm/m].

5. Conclusion

This study dealt with the process of obtaining the optimization model in the design of the 78 kW permanent-magnet synchronous generator (PMSG) driven by an engine. For this, 1800 rpm, the nominal rotation speed of an engine, was selected, and the generator that can provide the maximum output despite its small size was designed to ensure a 460 Nm torque.

To determine the number of poles, the characteristics of the 4- and 8-pole models were identified using FEA (finite-element analysis) and a d,q-axis equivalent circuit. The space harmonic was used in determining the number of slots, and 42 slots were determined as the number of slots. The 4-pole model with 42 slots and the 8-pole model with 42 slots were compared. As a result of the analysis using FEA, the 4-pole model showed relatively low iron loss and EMF THD values. On the other hand, the inductance of the 4-pole model turned out to be relatively higher than that of the 8-pole model, and the power density of the former was also higher. The voltage regulation of the 4-pole model was found to be relatively larger than that of the 8-pole model. Based on the judgment that the 4-pole model will be superior if the aim is to improve the power density, the number of poles was determined to be 4. The process of selecting the number of poles revealed that 42 slots were the most excellent in all the aspects, such as the no-load-induced voltage, EMF THD, and deformation of the stator, and thus, the number of slots was determined to be 42.

The voltage regulation and inductance of the 4-pole model had to be reduced to obtain the optimum model. Accordingly, the changes in the inductance and efficiency according to the *TRV* and *SR* were investigated through the sizing optimization technique. To ensure that the flux density of the rotor core is less than 1.5 T, the rotor outer diameters were limited to more than 200 mm. The final conclusion derived considering the efficiency, temperature, and inductance was that the point where the *SR* is 1.75 and the *TRV* is 42 is the best. In the sizing optimum point, the inductance was decreased by about 30 % compared to the initial model, and subsequently, the voltage regulation was improved by 7.8 %.

Acknowledgement

This study is a research project (No. 20152010103580) conducted with the support of Korea Institute of Energy Technology Evaluation and Planning (KETEP) and funded by the Ministry of Trade, Industry, and Energy in 2016.

References

[1] A. Elmitwally and M. Rashed, IEEE Trans. Energy Conversion **26**, 1 (2011).
[2] W. J. Lee, H. J. Lee, and H. J. Cha, The Transactions of the Korean Institute of Electrical Engineers **63**, 10 (2014).
[3] T. J. Lee, J. M. Jo, C. H. Shin, and H. J. Cha, the Korean Institute of Power Electronics (2015) pp. 147-148.
[4] K. Kamiev, J. Nerg, J. Pyrhonen, V. Zaboin, and J. Tapia, IEEE Trans. Energy Conversion **28**, 4 (2013).
[5] H. Markiewicz and A. Klajn, Standard EN 50160-Voltage characteristics in public distribution systems, Power Quality Application Guide (2004).
[6] Lloyd's Register Rules and Regulations for the Classification of Ships **6**, 2 (2011).
[7] K. Kamiev, J. Pyrhönen, J. Nerg, Senior Member, V. Zaboin, and J. Tapia, Member, IEEE Trans. Energy Conversion **28**, 4 (2013).